Journal of Computational and Nonlinear Dynamics. Received November 15, 2016;
Accepted manuscript posted September 19, 2017. doi:10.1115/1.4037923

Non-Linear Analysis of Shape Memory Devices with Duffing and Quadratic Oscillators

Shantanu Rajendra Gaikward and Ashok Kumar Pandey*
Mechanical and Aerospace Engineering,
Indian Institute of Technology Hyderabad,
Kandi, Sangareddy-502285, Telangana, India.

Abstract

In this paper, we investigate the linear and nonlinear response of SMA based Duffing and Quadratic oscillator under large deflection conditions. In this study, we first present thermomechanical constitutive modeling of SMA with a single degree of freedom system. Subsequently, we solve equation to obtain linear frequency and nonlinear frequency response using the method of harmonic balance and validate it with numerical solution as well as averaging method under the isothermal condition. However, for non-isothermal condition, we analyze the influence of cubic and quadratic nonlinearity on nonlinear response based on method of harmonic balance. Analysis of results lead to various ways of controlling the nature and extent of nonlinear response of SMA based oscillators. Such findings can be effectively used to control external vibration of different systems.

1 Introduction

Shape memory alloy (SMA) has been used to control vibration in various areas such as aerospace, buildings, bridges, automobile, biotechnology, etc, as its behavior and response can be controlled under various operating conditions. A typical SMA material shows pseudoelastic or superelastic behavior, in which, for a given external loading, its internal temperature changes with deformation due to phase transformation and heat exchange with surrounding. The phase transformation between austenite (A) at higher temperature and martensite (M) at lower temperature can induce an exothermic A $\rightarrow$ M as well as endothermic M $\rightarrow$ A transformations due to loading and unloading, respectively. Figure 1(a) shows the structure of phase transformation between austenite to martensite state. Figure 1(b) shows a detailed hysteresis loop due to internal changes in phase and temperature of SMA. It shows that during the cooling process, austenite state (A) is converted into twinned martensite (B) where the process of martensite transformation initiates. It is transformed into final state of detwinned martensite phase (C) under loading. After releasing the load, material regains its shape through a linear process until the stress becomes zero (D). At point D, the process of transformation to austenite state commences. Due to heating

*Address all correspondence to this author. E-mail: ashok@iith.ac.in

process, such transformation completes at point F which is called austenite phase. Figure 1(c) shows the effect of loading rate on hysteresis loop of SMA. It shows different types of responses under slow and fast loading and associated effects on slopes of hysteresis loops. If the loading rate is slow, temperature variations are small, hence system shows isothermal condition. Consequently, isothermal hysteresis loop is almost flat and two plateaus are parallel. For a faster loading rate under non-isothermal condition, nearly flat plateaus become steeper and the area of hysteresis loop is reduced. Therefore, to model a mechanical oscillator with SMA under external dynamic loading, rate of loading needs to be taken into consideration. In this paper, we discuss the response of an SMA based oscillator with linear and nonlinear stiffness under isothermal as well as non-isothermal conditions.

Research related to the development of SMA material and tuning of its properties with new alloy for various applications covers a wide range of problems. Dimitris [6] has discussed modeling of SMA along with its application and properties in great detail. Pseudoelastic model of SMA is described vividly by Bernardini and Vestroni [1] using the single degree of freedom system. Many systems incorporating SMA based cantilever beams are also widely studied [1–3]. To study thermomechanical behavior of SMA based system, the deformation, phase transformation and temperature variation are captured by governing equation along with constitutive equations of SMA. Constitutive equations governing hysteresis model are obtained using a free energy function as explained by Bernardini [4], and Ivshin and Pence [5] for isothermal as well as non-isothermal conditions. The isothermal condition neglects heat transfer with the surrounding [2]. Moussa et al. [7] presented experimental as well as theoretical studies of thermomechanical behaviour of superelastic shape memory alloys for quasi-static loading cases. Theoretical and experimental studies of SMA based systems are also studied in variety of structures [8, 19, 21]. Nonlinear frequency response of displacement amplitude as well as temperature in SMA based system is obtained by solving coupled equation using the method of harmonic balance and the averaging method, [9, 10]. In addition to the model developed by [1], another micromechanical model is also developed by the Oberaigner et al. [20]. It consists of a kinetic equation, stress-strain relation, temperature-transformed and volume-fraction relations. These equations couple heat conduction and vibration of a rod. Changes in the phase of the material lead to energy dissipation. Applying this model, a working temperature of damping can be found which lies between the temperatures of martensite start and martensite finish. Thermodynamics of two models of pseudoelastic behavior of SMA have been developed by Raniecki et al. [22]. The first model, R-model, undergoes reversible process only and constitutes the Maxwell model of phase transformation. Second model, RL-model, includes interaction of energy. It determines formation of external and internal hysteresis loops with the Clausius-Duhem inequality.

Although, there are numerous studies available to analyze the influence of nonlinear frequency response of SMA based oscillator, but all of them consider nonlinearity directly associated with SMA behavior. In this paper, we study the influence of cubic and quadratic nonlinearity arising from axial extension due to bending of SMA based beam. To do the analysis, we first consider Duffing oscillator with cubic nonlinearity [13]. We solve the equation using method of harmonic balance. By varying the nature and strength of nonlinearity from softening to hardening [24], we obtain coupled response of SMA dased Duffing oscillator. Subsequently, we also analyze combined effect of cubic and quadratic nonlinearity [14] using the method of harmonic balance. Above analysis is valid for isothermal as well as non-isothermal conditions. To compare different solution methods, we also solve SMA based Duffing oscillator using the averaging method [16]

for isothermal condition. On comparing the results obtained from harmonic balance method and methods of averaging, we found that averaging method underestimates the solution due to numerical error [23]. The comparison of solution of Duffing oscillator with and without SMA shows that frequency tuning of SMA based response can be tuned effectively by varying the coefficients of Duffing and Quadratic oscillator.

2 Governing equation

In this section, we present the classical equations which govern thermomechanical behavior of SMA based oscillator as mentioned by Bernardini and Vestroni [1], Lacarbonara et al. [2], and Ivshin and Pence [5], respectively. In general, an SMA oscillator is modelled as a pseudoelastic oscillator containing mass m, damping coefficient μ, and a SMA rod exhibiting hysteresis behavior, as shown in Figure 2(a). Figure 2(b) shows description of heat exchange between the SMA with internal temperature ϑ and surrounding temperature ϑ_E. In this paper, we analyze the influence of additional nonlinearity such as cubic and quadratic nonlinearity in stiffness which may be introduced due to geometric nonlinearity. For the sake of clarity, we first present only classical model of SMA without these non-linearities in following paragraph.

For non-isothermal condition, temperature ϑ, displacement x, velocity v, and the fraction of martensite phase, $\xi \in [0,1]$ form a four dimensional state-space system [2], where, $\xi = 0$ represents a complete austensitic state (A) and $\xi = 1$ represents complete martensitic state (M). The effect associated with the material microstructure is captured by the material parameter $\delta = x_{(\xi=1)} - x_{(\xi=0)}$ with $\delta > 0$ which shows maximum transformation displacement [2, 5]. The governing equations for thermomechanical behavior of SMA consists of linear momentum equation, internal energy balance, entropy balance, and the second law of thermodynamics as [2]

$$m\ddot{x} = \gamma\cos(\Omega t) - f - \mu\dot{x} \tag{1}$$

$$\dot{e} = f\dot{x} + \dot{Q},\ \vartheta\dot{\eta} = \dot{Q} + \dot{\Gamma},\ \dot{\Gamma} \geq 0 \tag{2}$$

where, e denotes the internal energy, $\dot{Q}$ represents the rate of heat exchange with surrounding, $\dot{\Gamma} = \Pi\dot{\xi}$ indicates the rate of energy dissipation, $\eta = c\ln\frac{\vartheta}{\vartheta_0} - b\delta\xi - b_0$ gives entropy of the system, $f = K(x - \text{sgn}(x)\delta\xi)$ captures the restoring force of pseudoelastic SMA device. Here, $K > 0$ is defined as elastic stiffness, $c > 0$ as the heat capacity, b as the slope of temperature-transformation force plane, and b_0 as entropy of SMA device under the fully austensitic state at reference temperature ϑ_0, $\Pi = K\delta(|x| - \delta\xi) - b\delta(\vartheta - \vartheta_0)$ is the thermodynamic driving force associated with phase transformation rate $\dot{\xi}$. Equations (1) and (2) can be written in the state-space form in terms of state variables ($\hat{x}$, $\hat{v}$, ξ, $\hat{\vartheta}$) as [2]

$$\dot{\hat{x}} = \hat{v} \tag{3}$$

$$\dot{\hat{v}} = \hat{\gamma}\cos(\hat{\Omega}\hat{t}) - (\hat{x} - \text{sgn}(\hat{x})\lambda\xi) - 2\zeta\hat{v}, \tag{4}$$

$$\dot{\xi} = \frac{\hat{Z}_1}{1 - \hat{Z}_1\hat{Z}_2}[\text{sgn}(\hat{x})J\hat{v} + \hat{h}(\hat{\vartheta} - \hat{\vartheta_E})], \tag{5}$$

$$\dot{\hat{\vartheta}} = \frac{1}{1 - \hat{Z}_1\hat{Z}_2}[-\text{sgn}(\hat{x})J\hat{Z}_1\hat{Z}_2\hat{v} - \hat{h}(\hat{\vartheta} - \hat{\vartheta_E})]. \tag{6}$$

where, the non-dimensional variables defined in Eqns. (3)-(6) are given by

$$\hat{t} = \omega t, \quad \hat{x} = \frac{x}{x_{Ms}}, \quad \hat{\vartheta} = \frac{\vartheta}{\vartheta_r}, \tag{7}$$

$$\hat{G} = Gb\delta\vartheta_r = \begin{cases} \hat{k_1}(1-\xi)[1+\tanh(\hat{k_1}\hat{\Pi}+\hat{k_2})], & \text{if } \dot{\xi} > 0 \\ \hat{k_3}\xi[1-\tanh(\hat{k_3}\hat{\Pi}+\hat{k_4})], & \text{if } \dot{\xi} < 0 \end{cases} \tag{8}$$

$$\hat{\Pi} = J(|\hat{x}| - \lambda\xi) - (\hat{\vartheta} - \hat{\vartheta_0}) \tag{9}$$

$$\hat{Z_1} = \frac{\hat{G}}{1+\lambda J\hat{G}}, \quad \hat{Z_2} = -L[J(|\hat{x}| - \lambda\xi) + \hat{\vartheta_0}], \tag{10}$$

where, ω and other non-dimensional parameters defined in Eqns. (7)-(10) are

$$\omega = \sqrt{\frac{K}{m}}, \quad \lambda = \frac{\delta}{x_{Ms}}, \quad L = \frac{b\delta}{c}, \quad \hat{h} = \frac{h}{c\omega}, \quad J = \frac{f_{Ms}}{b\vartheta_r}, \tag{11}$$

$$\zeta = \frac{\mu}{2\omega m}, \quad \hat{\gamma} = \frac{\gamma}{f_{Ms}}, \quad \hat{\Omega} = \frac{\Omega}{\omega}, \quad \hat{k_j} = k_j b\delta\vartheta_r, \quad j = 1, 3 \tag{12}$$

such that $\hat{k}'s$ are given by

$$\hat{k_1} = \frac{2r}{J(\hat{q_1}-1)}, \quad \hat{k_2} = k_2 = \frac{2(1-\hat{\vartheta_0}) - J(\hat{q_1}+1)}{J(\hat{q_1}-1)}r \tag{13}$$

$$\hat{k_3} = \frac{2r}{(1-\hat{q_2})\hat{q_3}J}, \quad \hat{k_4} = k_4 = \frac{2(1-\hat{\vartheta_0}) - \hat{q_3}J(\hat{q_2}+1)}{(1-\hat{q_2})\hat{q_3}J}r, \tag{14}$$

where, k_1 regulates the slope of phase fraction evolution and k_2 controls the actual value of Π when the transformation takes place both under forward process $M \to A$; k_3 and k_4 are corresponding values under reverse process of transformation $A \to M$; $\hat{q_1} = \frac{f_{\mathrm{Mf}}}{f_{\mathrm{Ms}}}$, $\hat{q_2} = \frac{f_{\mathrm{Af}}}{f_{\mathrm{As}}}$, $\hat{q_3} = \frac{f_{\mathrm{As}}}{f_{\mathrm{Ms}}}$; f_{Ms}, f_{Mf}, f_{As}, and f_{Af} are forces at the start and finish of corresponding transformations at temperature ϑ_r; $\hat{q_2} = (1+\hat{q_3}-\hat{q_1})/\hat{q_3}$ and $r = \tanh^{-1}(1-2\xi_r)$ with ξ_r is residue remaining during phase transformation. For more details, reader is advised to refer Lacarbonara *et al.* [2] . For solving Eqns.(3)-(6), we provide the parameters defined in Eqns. (11)-(14) and zero initial conditions for state variables ($\hat{x}$, $\hat{v}$, ξ, $\hat{\vartheta}$). Similarly, for isothermal condition, dimension of the system is reduced to three, i.e., ($\hat{x}$, $\hat{v}$, ξ), as the variation of internal temperature is neglected.

2.1 SMA based Duffing oscillator under non-isothermal conditions

To describe the influence of cubic non-linearity due to large deflection, we include a cubic non-linear stiffness term in the equations governing $\hat{x}$, $\hat{\vartheta}$ and $\hat{\xi}$, respectively. Neglecting hat for the sake of simplicity and rearranging equations, we write the form of SMA based Duffing oscillator as

$$\ddot{x} = \gamma\cos(\Omega t) - (x - \mathrm{sgn}(x)\lambda\xi) - 2\zeta\dot{x} - \beta_0 x^3, \tag{15}$$

$$\dot{\vartheta} = h(\vartheta_E - \vartheta) - Z_2\dot{\xi}, \tag{16}$$

where, β_0 is the coefficient of cubic stiffness term.

To investigate the response of device, we plot frequency response curves for both displacement and temperature under non-isothermal condition for β_0 varying from -0.1 to 1.1. To obtain the nonlinear frequency response of SMA based Duffing oscillator, we solve above equation using harmonic balance method. For continuation of stable branch, we use arc-continuation method with secant predictor [1, 9, 10]. The solution procedure can be briefly described below.

Lets take

$$\mathbf{X} = \begin{bmatrix} \ddot{x} \\ \dot{\vartheta} \end{bmatrix} \tag{17}$$

and assume the solution of type

$$x = \frac{a_0}{2} + \sum_{i=1}^{N} A_n \cos(n\Omega t) + B_n \sin(n\Omega t) \qquad n = 1, 2....N \tag{18}$$

$$\vartheta = \frac{b_0}{2} + \sum_{i=1}^{N} C_n \cos(n\Omega t) + D_n \sin(n\Omega t) \qquad n = 1, 2....N. \tag{19}$$

Considering

$$L_1 = \gamma \cos(\Omega t) - (x - \mathrm{sgn}(x)\lambda\xi) - 2\zeta\dot{x} - \beta_0 x^3, \tag{20}$$

$$L_2 = h(\vartheta_E - \vartheta) - Z_2\dot{\xi}, \tag{21}$$

and using Eqns.(15), (16), (20) and (21), we get

$$\mathbf{X} = \begin{bmatrix} \ddot{x} \\ \dot{\vartheta} \end{bmatrix} = \begin{bmatrix} L_1 \\ L_2 \end{bmatrix}. \tag{22}$$

Assuming

$$L_1 = \frac{c_0}{2} + \sum_{i=1}^{N} E_n \cos(n\Omega t) + F_n \sin(n\Omega t) \qquad n = 1, 2....N \tag{23}$$

$$L_2 = \frac{d_0}{2} + \sum_{i=1}^{N} H_n \cos(n\Omega t) + I_n \sin(n\Omega t) \qquad n = 1, 2....N. \tag{24}$$

From sets of Eqns. (18), (19), (20), (21) (23) and (24), and using Galerkin approximation [9], we obtain the following harmonic balance equations,

$$E_n + A_n\Omega^2 = 0 \tag{25}$$

$$F_n + B_n\Omega^2 = 0 \tag{26}$$

$$H_n - D_n\Omega = 0 \tag{27}$$

$$I_n + C_n\Omega = 0. \tag{28}$$

In above sets of Eqns. (25)-(28), there are $4N$ unknowns (A_n, B_n, C_n and D_n) and $4N$ equations. The constants E_n, F_n, H_n and I_n depend on A_n, B_n, C_n and D_n. To calculate Fourier coefficient E_n, F_n, H_n and I_n, we use the iterative algorithm based on evolution of A_n, B_n, C_n and D_n. From A_n, B_n, C_n and D_n, we calculate the values of x and ϑ for timespan of $[0\ 2\pi]$. Using the values of x and ϑ, we obtain ξ using numerical integration. Subsequently, we compute the values of L_1 and L_2 using x, ϑ and ξ. Finally, the values of E_n, F_n, H_n and I_n are obtained by IFFT (Inverse Fast Fourier Transform).

To obtain frequency-response curve, we use continuation method. Here, the spherical arclength continuation method is used to obtained a constrained equation of the form,

$$(\mathbf{x} - \mathbf{x}_i)^T(\mathbf{x} - \mathbf{x}_i) - (\Delta s)^2 = 0. \tag{29}$$

Here, $\mathbf{x}$ is unknown quantity of current step and $\mathbf{x}_i$ known quantity of previous step. In above constrained equation, s is defined as the arclength along a curve and Δs is the step size. Subsequently, the predictor-corrector algorithm is used for iterative method. Here, the predictor algorithm is proposed as,

$$\mathbf{x}_{i+1} = \mathbf{x}_i + p_i(\mathbf{x}_i - \mathbf{x}_{i-1}), \tag{30}$$

where, p_i is the step-dependent parameter. For corrector algorithm, we use Newton-Raphson iterative method. Finally, by using predictor-corrector method, we obtain the values of unknown constant.

2.2 SMA based Duffing oscillator under Isothermal conditions

To investigate the response of SMA based Duffing oscillator under isothermal condition, internal temperature is taken as constant. Consequently, the governing equations given by Eqns.(15) and () are reduced to single equation as

$$\ddot{x} = \gamma\cos(\Omega t) - (x - \mathrm{sgn}(x)\lambda\xi) - 2\zeta\dot{x} - \beta_0 x^3. \tag{31}$$

Assuming

$$\mathbf{X} = [\ddot{x}] \tag{32}$$

and considering

$$L_1 = \gamma\cos(\Omega t) - (x - \mathrm{sgn}(x)\lambda\xi) - 2\zeta\dot{x} - \beta_0 x^3. \tag{33}$$

Writing $\mathbf{X}$ as,

$$\mathbf{X} = [\ddot{x}] = [L_1] \tag{34}$$

and assuming the Fourier series for x as,

$$x = \frac{a_0}{2} + \sum_{i=1}^{N} A_n \cos(n\Omega t) + B_n \sin(n\Omega t) \qquad n = 1, 2....N \tag{35}$$

$$L_1 = \frac{c_0}{2} + \sum_{i=1}^{N} E_n \cos(n\Omega t) + F_n \sin(n\Omega t) \qquad n = 1, 2....N. \tag{36}$$

Solving Eqns. (32), (34), (35) and (36), we obtain

$$E_n + A_n\Omega^2 = 0 \tag{37}$$

$$F_n + B_n\Omega^2 = 0. \tag{38}$$

In above Eqns. (37) and (38), there are $2N$ unknown (A_n and B_n), and $2N$ equations. Fourier coefficients E_n and F_n are dependent on A_n and B_n. To calculate Fourier coefficients E_n and F_n, we use iterative algorithm based on evolution of A_n and B_n. From Fourier coefficients of A_n and B_n, we calculate values of x for timespan of $[0\ \frac{2\pi}{\Omega}]$. In isothermal case, ϑ is constant. Using values of x and ϑ, we get the values of ξ using numerical integration. Subsequently, the value of L_1 is obtained using values of x and ξ. Finally, we calculate values of E_n and F_n by using IFFT (Inverse Fast Fourier Transform). In order to obtain an unstable branch of frequency response curve, we use arc continuation method as described in the previous section.

2.3 SMA based Duffing and quadratic oscillators

To investigate the combined effect of nonlinear cubic and quadratic stiffness on the response of SMA based Duffing and quadratic oscillators, Eqns. (15) and (16) modified to include quadratic nonlinear term $\beta_1 x^2$ to get the following equations

$$\ddot{x} = \gamma\cos(\Omega t) - (x - \mathrm{sgn}(x)\lambda\xi) - 2\zeta\dot{x} - \beta_0 x^3 - \beta_1 x^2, \tag{39}$$

$$\dot{\vartheta} = h(\vartheta_E - \vartheta) - Z_2\dot{\xi}, \tag{40}$$

where, β_1 is quadratic coefficient. To examine the system behavior, we vary β_1 for different values of β_0. While β_1 varies from -0.1 to 0.9 when β_0 is taken as -0.1, 0 and 0.1, separately. For the given parameters, above equations are solved using methods of harmonic balance and arc-continutation as described in the previous section.

3 Results and Discussions

In this section, we present and discuss the variation of frequency response curves of SMA based Duffing and quadratic oscillators. To do the analysis, we take parameters used in the constitutive equations from [1, 2]. The value of different parameters of Ni-Ti wire are taken as

$$\lambda = 7, \quad q_1 = 1.05, \quad q_3 = 0.6, \quad L = 0.124, \tag{41}$$

$$\xi_r = 0.2, \quad J = 0.315, \quad h = 0.08, \quad \zeta = 0.05. \tag{42}$$

The system is harmonically excited with low forcing magnitude of $\gamma = 0.2$ to induce small nonlinearity with excitation frequency of Ω as a control parameter. For a given Ω, frequency response curve is found by plotting the maximum value of displacement, $\| X \|$ (Euclidean norm) or $|X|$ (absolute value), and temperature, $\| T \|$ or $|T|$, respectively.

3.1 SMA based Duffing Oscillator under Isothermal Condition

In this section, we analyze transient and frequency response of SMA based Duffing oscillator given by Eqn.(31) under isothermal condition. Figure 3(a) shows a typical frequency response curve of SMA without Duffing nonlinearity, i.e., $\beta_0 = 0.0$, corresponding to forcing of $\gamma = 0.2$. It also shows two bifurcation points 'A' and 'B' at approximately $\Omega = 0.87$ and 0.84, respectively. Figures 3(b) and (c) show the variation non-dimensional pseudo-elastic force $f = (x - \text{sgn}(x)\lambda\xi)$ with displacement and the transient response of displacement corresponding to points 'A' and 'B'. Figure 3(d) show FFT of the time series of displacement containing a single frequency for both the points. Figures 3(e) and (f) show phase diagrams and Poincare maps which confirm the presence of a periodic solution for two points corresponding to non-dimensional angular frequencies of $\Omega = 0.87$ and 0.84. Now, we compare the frequency response curves obtained from the method of harmonic balance, method of averaging [16], and the numerical solution. The method of harmonic balance is described in detail in the previous section and method of averaging [16] is described in Appendix A for SMA based Duffing oscillator under isothermal condition. In Figure 4(a), the solid curve represents solution by the method of averaging and dash curve represents that by harmonic balance method when $\beta_0 = 0$ and $\gamma = 0.2$. Such variations are confirmed when the results are compared with numerical solution obtained using Runge-Kutte integration under forward and backward frequency sweep. To compare the solution for non-zero values of β_0 varying from -0.1 to 1.1, results obtained by methods of harmonic balance and averaging show similar variations as shown in Fig. 4(b). Based on the results, it is found that using higher values of geometric nonlinearity, the nature of nonlinearity in SMA based Duffing oscillator can be changed from softening to hardening. Such a large tuning in nonlinear frequency response can be utilized to control the vibration effectively. Figure 4(c) show the stable and unstable curves of frequency response obtained using averaging method at various values of nonlinear stiffness $beta_0$. To analyze the curve, we divide a typical frequency response into five regions OA, AB, BC, CD, DE, and EF, respectively as shown in Figure 4(a). For $\beta_0 = -0.1$, AB curve represent unstable curve. As $\beta_0 = 0.0$ and 0.1, unstable portion reduces and it diminish at $\beta = 0.2$. With further increase of β_0 value from 0.3 to 0.6, unstable portion DE increases. After $\beta_0 = 0.7$, portion CD also becomes unstable. Hence, for $\beta_0 = 0.8$ and 1.1, portion CDE shows unstable solution similar to the solutions of Duffing equation. Beyond $\beta_0 = 1.1$, Duffing response subsidize the non-linear effect of pseudo-elastic force of SMA. In the subsequent sections, we discuss in detail about such variation in the frequency response curve under non-isothermal conditions using the method of harmonic balance.

3.2 SMA based Duffing Oscillator under Non-Isothermal Condition

The SMA based systems under non-isothermal conditions usually show nonlinear softening effect in the frequency response curve in displacement as well as temperature. Figure 5(a) shows the comparison between numerical solution and solution using the method of harmonic balance for SMA. In this case, nonlinear effect is induced mainly due to hysteresis, i.e., energy dissipation characteristics, which causes phase transformation and energy exchange with the surrounding. When SMA based oscillator is combined with Duffing oscillator in which nonlinear stiffness is induced due to large deformation of the material, it starts increasing the hardening nature. Figure 5(a) shows the comparison between nonlinear frequency response of Duffing oscillator with and without SMA for β_0 varying from -0.09 to 1.1. It shows that due to effect of cubic nonlinearity in the stiffness of SMA based Duffing oscillator, the nature of nonlinearity can be effectively changed to hardening type. Figures 5(c) and (d) show the frequency response curve of displacement and temperature change due to change in nonlinearity. However, it is also found that the magnitude of displacement, $\| X \|$, as well as temperature, $\| T \|$, reduce with increase in nonlinearity coefficient, β_0. On the other hand, if the sign of β_0 is reversed, softening nature of the tube increases even further. For $\beta_0 = 0.1$, frequency response curve shows very small non-linearity, and for $\beta_0 = 0.2$, bifurcation point disappears for softening curve and it shows only stable solution. For $\beta_0 = 0.3$, the curve becomes hardening type with small non-linearity. A further increase of β_0 value leads to more hardening type non-linearity. Thus, the higher values of β_0 means increase of $\| X \|$ and $\| T \|$ with frequency. After bifurcation point, values of $\| X \|$ and $\| T \|$ decrease with decrease in frequency. At $\beta_0 = 1.1$, frequency response curve shows little effect of SMA damping and full dominance of nonlinearity in stiffness of Duffing oscillator. Finally, it is found that the sign and strength of β_0 can be tuned to either increase or decrease the SMA effect.

3.3 SMA based Duffing and Quadratic Oscillator under Non-Isothermal Condition

Similarly to the previous section, we also discuss the influence of quadratic nonlinearity with and without cubic nonlinearity in SMA based Duffing and quadratic oscillator under non-isothermal condition. To do the analysis, we use the same parameters of SMA as mentioned in the previous section. However, the quadratic nonlinear parameters, β_1, are taken from -0.1 to 0.9 when the cubic nonlinear parameter β_0 are -0.1, 0, and 0.1. Figures 6(a) and (b) show the frequency response curves for displacement and temperature at different values of cubic and quadratic nonlinear stiffness of SMA based Duffing and quadratic oscillator. For a fixed and non-zero values of cubic coefficient, the nonlinear response shows combined effect of cubic and quadratic nonlinearity. For zero value of β_0, the curve shows only quadratic effect. Analysis of displacement and temperature response shows that the quadratic nonlinearity helps in tuning the nature of nonlinear response but its strength is small as compared to that due to cubic nonlinearity. Additionally, the displacement response also shows the presence of superharmonic response of the order 2 and 3, respectively,

At the end, we state that the cubic nonlinear stiffness which may be induced due to large deformation of SMA beam can lead to frequency tuning for a large range. Hence, the vibration of different frequencies can be controlled using SMA based system. Although, the saddle-node

bifurcation is observed corresponding to excitation forcing of $\gamma = 0.2$ at different $beta_0$, the possibility of quasiperiodic and chaotic responses can also be probed at higher excitation forcing.

4 Conclusions

In this paper, we analyzed the influence of cubic and quadratic nonlinear stiffness on the response of SMA based Duffing and quadratic oscillator under isothermal and non-isothermal conditions. To do the analysis, we solved governing equation using method of harmonic balance, method of averaging and compared the solutions with numerical integration under isothermal condition. All the solutions were found to be closer to each other. To do further analysis under non-isothermal condition, we used the method of harmonic balance. After validating it with numerical solution, we varied nonlinear stiffness parameter , β_0, from -0.09 to 1.1 in Duffing oscillator with and without SMA. It was observed that SMA based oscillator not only reduces the displacement amplitude effectively but it can also be used to tune the nature of nonlinearity from softening to hardening. Over the same range of β_0, the temperature change is also found to be decreased, effectively. Similar variation was also observed due to change in quadratic nonlinearity, β_1, in SMA based quadratic and Duffing oscillator. However, the strength of change due to quadratic nonlinearity is found to be less than that due to cubic nonlinearity. However, it leads to the presence of super harmonic response in addition to primary resonance response.

Appendix A. SMA Based Duffing Oscillator for Isothermal Case using the Method of Averaging

In this section, we describe the Krylov−Bogolyubov method of averaging [16] to solve SMA based Duffing oscillator under isothermal condition. Neglecting the temperature variation, governing equation is reduced to

$$\ddot{x} = \gamma\cos(\Omega t) - (x - \mathrm{sgn}(x)\lambda\xi) - 2\zeta\dot{x} - \beta_0 x^3.$$

Taking $f(x,\vartheta) = (x - \mathrm{sgn}(x)\lambda\xi + \beta_0 x^3)$, the above equation becomes

$$\ddot{x} = \gamma\cos(\Omega t) - f(x,\vartheta) - 2\zeta\dot{x}. \tag{43}$$

Assuming the solution as $x = R\cos(\Omega t + \Phi)$, where R is the amplitude and Φ is the phase, and both are slowly varying function of time, and considering $\theta = \Omega t + \Phi$, we get

$$x = R\cos(\Omega t + \Phi) = R\cos(\theta). \tag{44}$$

Differentiating Eq. (44) with respect to time, we get

$$\dot{x} = \dot{R}\cos(\Omega t + \Phi) - \Omega R\sin(\Omega t + \Phi) - \dot{\Phi}R\sin(\Omega t + \Phi)$$

or,

$$\dot{x} = \dot{R}\cos(\theta) - \Omega R\sin(\theta) - \dot{\Phi}R\sin(\theta) \quad . \tag{45}$$

Taking

$$\dot{R}\cos(\theta) - \dot{\Phi}R\sin(\theta) = 0, \tag{46}$$

Eqn. (45) becomes

$$\dot{x} = -\Omega R sin(\theta). \tag{47}$$

Again, differentiating Eq. (47) with respect to time, we get

$$\ddot{x} = -\Omega\dot{R}\sin(\Omega t + \Phi) - \Omega^2 R\cos(\Omega t + \Phi) - \dot{\Phi}R\sin(\Omega t + \Phi),$$

or,

$$\ddot{x} = -\Omega\dot{R}\sin(\theta) - \Omega^2 R\cos(\theta) - \dot{\Phi}R\sin(\theta). \tag{48}$$

Substituting Eqn. (47) and Eqn. (48) in Eqn. (43), we get

$$-\Omega\dot{R}\sin(\theta) - \Omega^2 R\cos(\theta) - \dot{\Phi}R\sin(\theta) + f(x,\vartheta) - 2\Omega\zeta R\sin(\theta) = \gamma\cos(\Omega t). \tag{49}$$

Solving Eqn. (46) and Eqn. (49) for $\dot{R}$ and $\dot{\Phi}$, we obtain

$$\dot{R} = \frac{-\gamma\cos(\Omega t)\sin(\theta)}{\Omega} - \Omega R\sin(\theta)cos(\theta) - 2\zeta R\sin^2(\theta) + \frac{f(x,\vartheta)\sin(\theta)}{\Omega} \tag{50}$$

$$\dot{\Phi} = \frac{-\gamma\cos(\Omega t)\cos(\theta)}{\Omega R} - \Omega\cos^2(\theta) - 2\zeta\sin(\theta)\cos(\theta) + \frac{f(x,\vartheta)\cos(\theta)}{\Omega R}. \tag{51}$$

Equations (50) and (51) can be averaged over one cycle of θ. Since, R and Φ are slowly varying functions as compared to θ, therefore, R and Φ are considered as constants. Consequently, we get the averaged equations as

$$\dot{R} = \frac{1}{2\pi}\int_0^{2\pi}\left(\frac{-\gamma\cos(\Omega t)\sin(\theta)}{\Omega} - \Omega R\sin(\theta)\cos(\theta) - 2\zeta R\sin^2(\theta) + \frac{f(x,\vartheta)\sin(\theta)}{\Omega}\right)d\theta \tag{52}$$

and

$$\dot{\Phi} = \frac{1}{2\pi}\int_0^{2\pi}\left(\frac{-\gamma\cos(\Omega t)\cos(\theta)}{\Omega R} - \Omega\cos^2(\theta) - 2\zeta\sin(\theta)\cos(\theta) + \frac{f(x,\vartheta)\cos(\theta)}{\Omega R}\right)d\theta \tag{53}$$

Equations (52) and (53) are reduced to

$$\dot{R} = \frac{-\gamma sin(\Phi)}{2\Omega} - \zeta R + \frac{1}{2\pi}\int_0^{2\pi} \left(\frac{f(x,\vartheta)sin(\theta)}{\Omega} \right) d\theta \tag{54}$$

$$\dot{\Phi} = \frac{-\gamma \cos(\Phi)}{2\Omega R} - \frac{\Omega}{2} + \frac{1}{2\pi}\int_0^{2\pi} \left(\frac{f(x,\vartheta)\cos(\theta)}{\Omega R} \right) d\theta. \; . \tag{55}$$

To obtain frequency response of R and Φ, we apply equilibrium conditions $\dot{R} = 0$ and $\dot{\Phi} = 0$. For solving equilibrium equations, we assume the Fourier series as,

$$f(x,\vartheta) = \frac{y_0}{2} + \sum_{i=1}^{N} U_n \cos(n\Omega t) + V_n sin(n\Omega t) \qquad n = 1, 2....N$$

or,

$$f(x,\vartheta) = \frac{y_0}{2} + \sum_{i=1}^{N} U_n \cos(n(\theta - \Phi)) + V_n sin(n(\theta - \Phi)) \; n = 1, 2....N. \tag{56}$$

Substituting Eqn. (56) in Eqns. (54) and (55) and performing integration, we get equilibrium equations in terms of Fourier coefficients U_n and V_n. To calculate these Fourier coefficients, we use iterative algorithm based on the values of R and Φ. From the values of R and Φ,we compute the values of x for timespan of $[0 \; \frac{2\pi}{\Omega}]$. In isothermal case, ϑ is constant. Using the values of x and ϑ, we obtain value of ξ by using numerical integration. Consequently, the values of $f(x,\vartheta)$ can be obtained for given values of x, ϑ and ξ. Finally, U_n and V_n can be computed using IFFT (Inverse Fast Fourier Transform). In order to obtain an unstable branch of frequency response curve, we used arc continuation method as described in the paper. The stability of the equilibrium solution can also be obtained based on eigenvalues of the Jacobian matrix defined as

$$J = \begin{bmatrix} \frac{\partial \dot{R}}{\partial R} & \frac{\partial \dot{R}}{\partial \phi} \\ \frac{\partial \dot{\phi}}{\partial R} & \frac{\partial \dot{\phi}}{\partial \phi} \end{bmatrix} = \begin{bmatrix} -\zeta & -\frac{\gamma\cos(\phi) - E_1\cos(\phi) + F_1\sin(\phi)}{2\omega} \\ \frac{\gamma\cos(\phi) - E_1\cos(\phi) + F_1\sin(\phi)}{2\omega R^2} & \frac{\gamma\sin(\phi) - E_1\sin(\phi) - F_1\cos(\phi)}{2\omega R} \end{bmatrix}. \tag{57}$$

The equilibrium solution (R, ϕ) is stable if real part of the eigenvalues, λ, of J are negative, i.e., Re(λ)=Trace(J)/2= $\frac{-2\zeta\omega R + \gamma\sin(\phi) - E_1\sin(\phi) - F_1\cos(\phi)}{4\omega R} < 0$. The bifurcation point is obtained from Re(λ)=0; Alternatively, we can also obtain the bifurcation point by finding sign of the slope of response curve R with respect to frequency using finite difference method.

Acknowledgment

The authors would like to thank Mr. P Manoj of IIT Hyderabad for reproducing the results of this paper.

References

[1] Bernardini, D., & Vestroni, F. (2003). Non-isothermal oscillations of pseudoelastic devices. International Journal of Non-Linear Mechanics, 38(9), 1297-1313.

[2] Lacarbonara, W., Bernardini, D., & Vestroni, F. (2004). Nonlinear thermomechanical oscillations of shape-memory devices. International Journal of Solids and Structures, 41(5), 1209-1234.

[3] Bernardini, D. & Rega, G. (2010). The influence of model parameters and of the thermomechanical coupling on the behavior of shape memory devices. International Journal of Non-Linear Mechanics, 45(10), 933-946.

[4] Bernardini, D. (2001). On the macroscopic free energy functions for shape memory alloys. Journal of the Mechanics and Physics of Solids, 49(4), 813-837.

[5] Ivshin, Y., & Pence, T. J. (1994). A thermomechanical model for a one variant shape memory material. Journal of intelligent material systems and structures, 5(4), 455-473.

[6] Dimitris, C. L. (2008). Shape memory alloys: Modeling and engineering applications. Springer-Verlag, US.

[7] Moussa, M. O., Moumni, Z., Doar, O., Touz, C., & Zaki, W. (2012). Non-linear dynamic thermomechanical behaviour of shape memory alloys. Journal of Intelligent Material Systems and Structures, 23(14), 1593-1611.

[8] Salichs, J., Hou, Z., & Noori, M. (2001). Vibration suppression of structures using passive shape memory alloy energy dissipation devices. Journal of Intelligent Material Systems and Structures, 12(10), 671-680.

[9] Urabe, M. (1965). Galerkin's procedure for nonlinear periodic systems. Archive for Rational Mechanics and Analysis, 20(2), 120-152.

[10] Nayfeh, A. H., & Balachandran, B. (1995). Applied nonlinear dynamics: analytical, computational, and experimental methods. In Wiley Series in Nonlinear Sciences. John Wiley & Sons, Inc New York.

[11] Ge, G. (2014). Response of a Shape Memory Alloy Beam Model under Narrow Band Noise Excitation. Mathematical Problems in Engineering, 2014, 985467, 1-7.

[12] Otsuka, K. & Wayman, C. M. (1999). Shape memory materials, Cambridge university press.

[13] Kovacic, I. & Brennan, M. J. (2011). The Duffing equation: nonlinear oscillators and their behaviour. John Wiley & Sons.

[14] Hu, H. (2006). Solution of a quadratic nonlinear oscillator by the method of harmonic balance. Journal of Sound and Vibration, 293(1), 462–468.

[15] Cveticanin, L. (2004). Vibrations of the nonlinear oscillator with quadratic nonlinearity. Physica A: Statistical Mechanics and its Applications, 341, 123-135.

[16] Krylov, N. & Bogoliubov, N. (1949). Introduction to Non-Linear Mechanics. Princeton University Press, London.

[17] Vestroni, F. & Capecchi, D. (1999). Coupling and resonance phenomena in dynamic systems with hysteresis. IUTAM Symposium on New Applications of Nonlinear and Chaotic Dynamics in Mechanics, Springer, 203–212.

[18] Saadat, S., Salichs, J., Noori, M., Hou, Z., Davoodi, H., Bar-On, I., Suzuki, Y. & Masuda, A. (2002). An overview of vibration and seismic applications of NiTi shape memory alloy. Smart materials and structures, 11(2), 218.

[19] Thomson, P., Balas, G. J., & Leo, P.H. (1995). The use of shape memory alloys for passive structural damping. Smart Materials and Structures, 4(1), 36.

[20] Oberaigner, E.R., Tanaka, K. & Fischer, F.D. (1996). Investigation of the damping behavior of a vibrating shape memory alloy rod using a micromechanical model. Smart materials and structures, 5(4), 456.

[21] Clark, P. W., Aiken, I. D., Kelly, J. M., Higashino, M. & Krumme, R. (1995).Experimental and analytical studies of shape-memory alloy dampers for structural control. Smart Structures and Materials, 241–251.

[22] Raniecki, B and Lexcellent, Ch & Tanaka, K (1992). Thermodynamic models of pseudoelastic behaviour of shape memory alloys. Archiv of Mechanics, Archiwum Mechaniki Stosowanej, 44, 261-284.

[23] Stoer, J. & Bulirsch, R. (2013). Introduction to numerical analysis. Springer Science & Business Media, 12.

[24] Nayfeh, A. H. & Sanchez, N. E. (1989). Bifurcations in a forced softening Duffing oscillator. International Journal of Non-Linear Mechanics, 24(6), 483-493.

List of Figures

Journal of Computational and Nonlinear Dynamics. Received November 15, 2016;
Accepted manuscript posted September 19, 2017. doi:10.1115/1.4037923

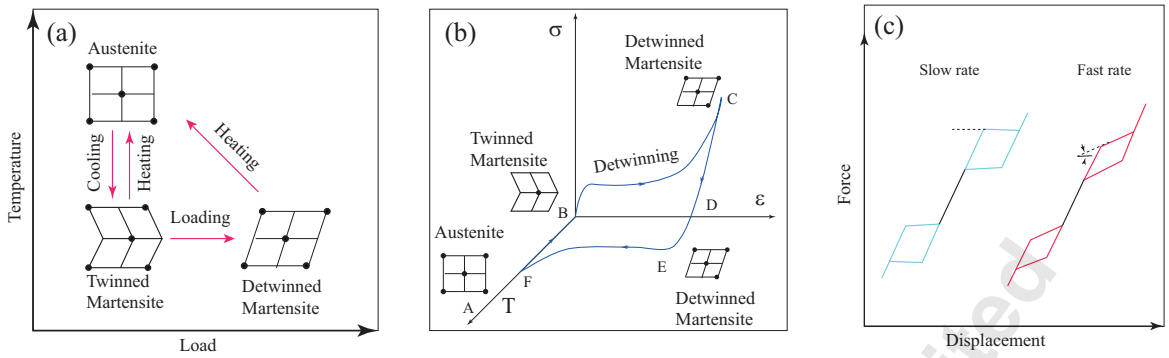

Figure 1: (a) Phase transformation of a SMA under loading and temperature effect; (b) Stress-strain-temperature hysteresis loop of a SMA; (c) Hysteresis loop at different loading rates.

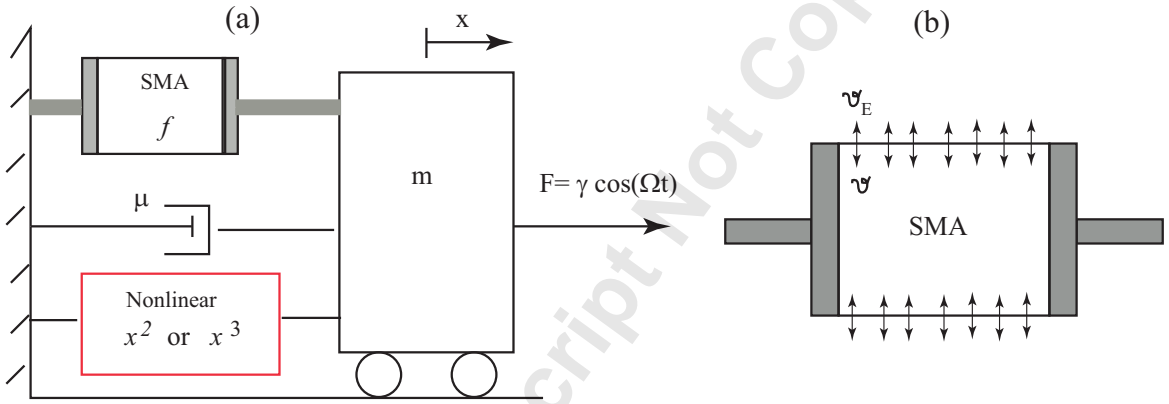

Figure 2: (a) A lumped model of SMA based oscillator including cubic and quadratic nonlinear stiffness. (b) A schematic representation of SMA with internal temperature and surrounding temperature.

Journal of Computational and Nonlinear Dynamics. Received November 15, 2016;
Accepted manuscript posted September 19, 2017. doi:10.1115/1.4037923

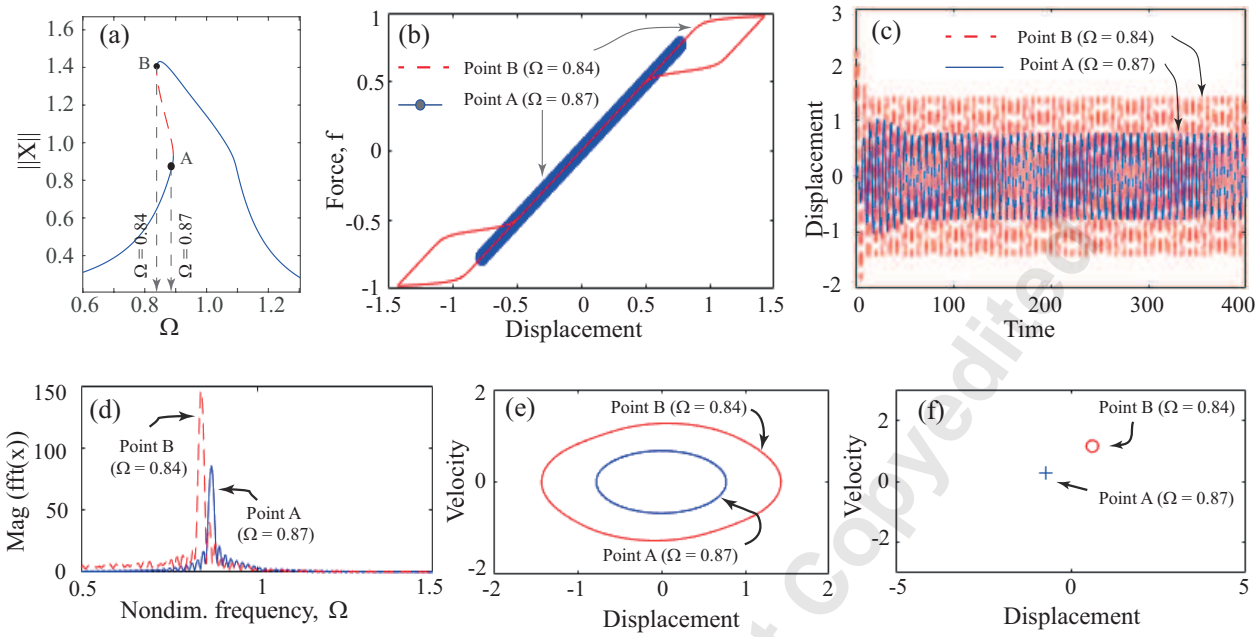

Figure 3: (a) Frequency response of SMA under isothermal condition with $\gamma = 0.2$ and $\beta_0 = 0.0$ showing the birfuaction points 'A' at $\Omega = 0.87$ and 'B' at $\Omega = 0.84$; (b) Variation of non-dimensional pseudoelastic force $f = (x - \text{sgn}(x)\lambda\xi)$ of SMA versus displacement, (b) Time history of displacement, (c) FFT of displacement signals, (d) Phase diagram and (e) Pincare map of signals under isothermal condition for points 'A' and 'B'.

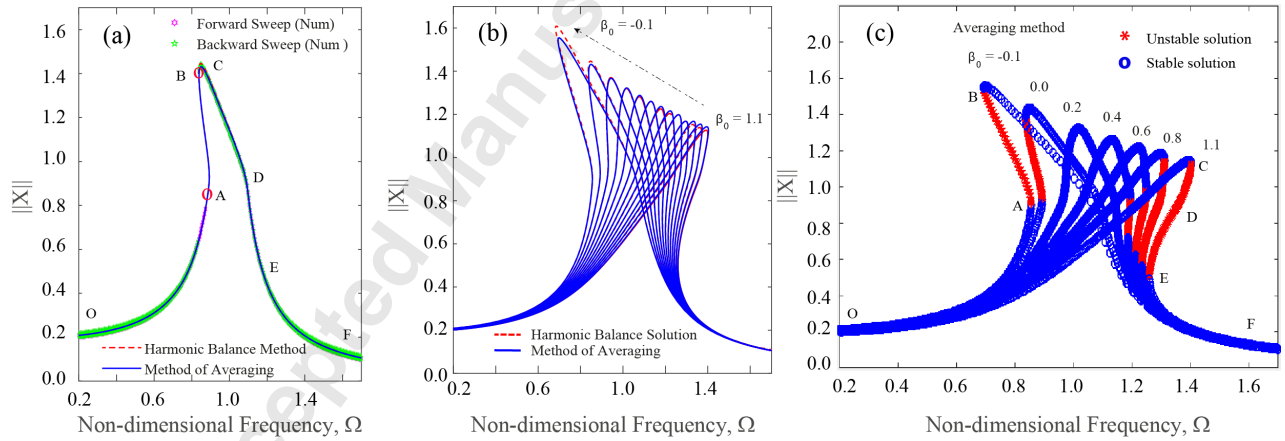

Figure 4: (a) Validation of solutions based on harmonic balance method and method of averaging under isothermal case with the numerical solution when $\beta_0 = 0$. Here, OA, AB, BC, CD, DE, EF indicate different portions of response curve; AB is unstable portion and rest of the portions are stable. (b) Comparison of the frequency response curves of SMA based cubic oscillator obtained from harmonic balance method and method of averaging under the isothermal condition when ($\gamma = 0.2$) and β_0 varies from -0.1 t0 1.1.(c) Unstable (red asterisk) and stable portions (blue circle) are shown for frequency response curves at different values of β_0.

Journal of Computational and Nonlinear Dynamics. Received November 15, 2016;
Accepted manuscript posted September 19, 2017. doi:10.1115/1.4037923

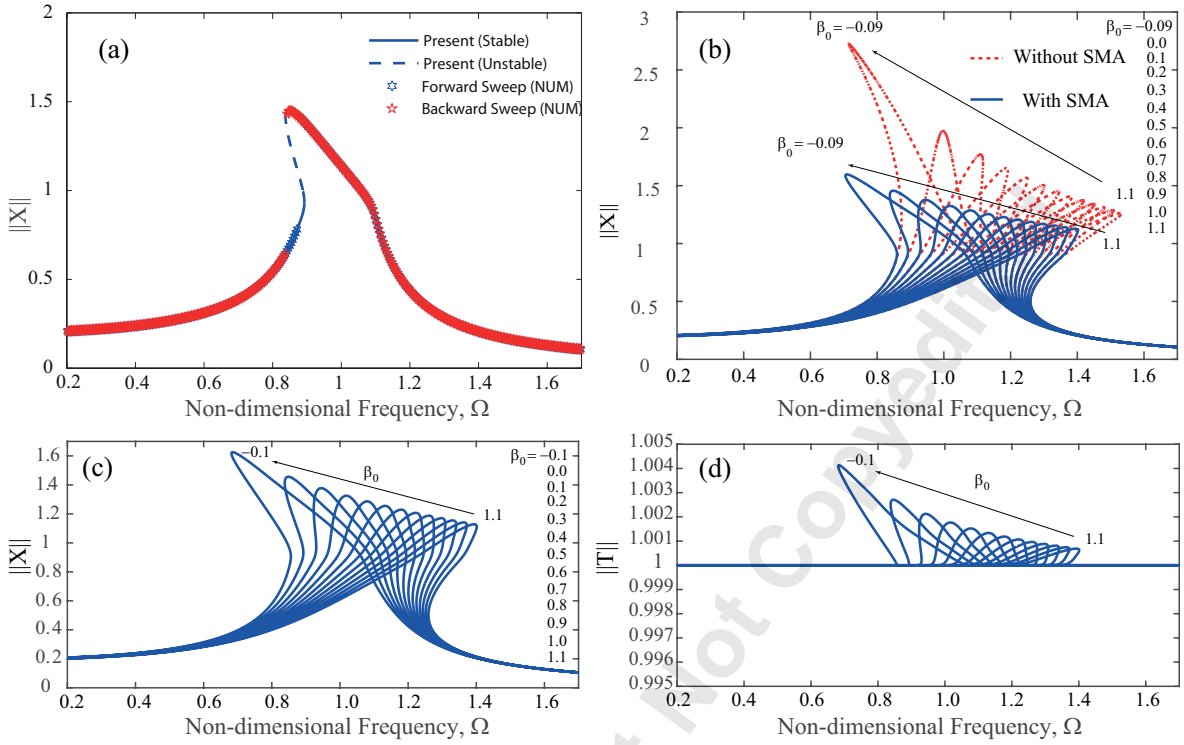

Figure 5: (a) Validation of solutions based on harmonic balance method with the numerical solution under non-isothermal condition when $\beta_0 = 0$; (b) Comparison of displacement based frequency response curves of Duffing oscillator with and without SMA at different values of non-linear constant β_0; Variation of (c) displacement and (d) temperature based frequency response curves for different values of β_0.

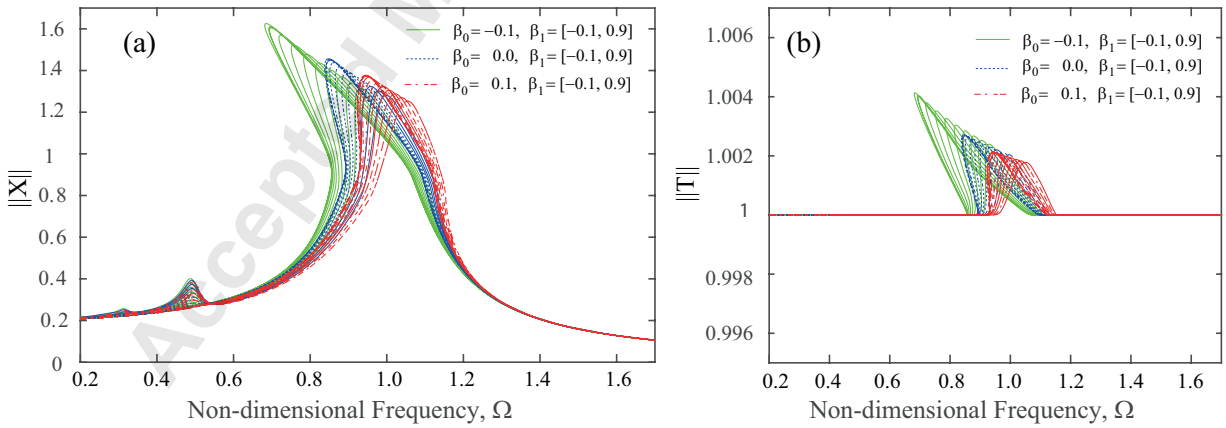

Figure 6: (a) Displacement frequency response curves and (b) Temperature frequency response curves of cubic and quadratic oscillator with SMA